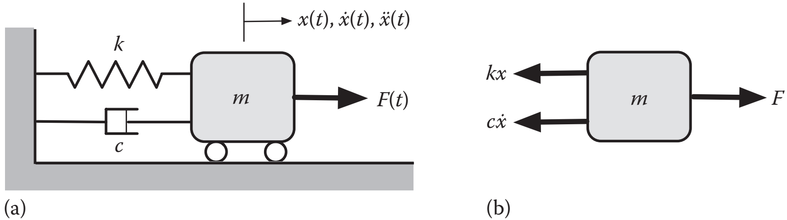

Figure 2.1 Damped SDOF system: (a) System parameters and loading and (b) free-body diagram.

002x001.eps

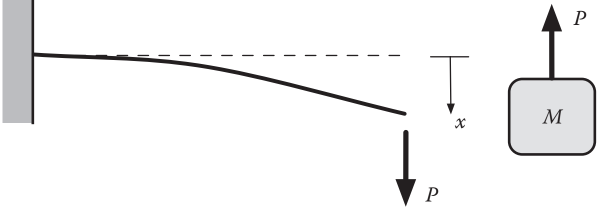

Figure 2.2 Free body diagrams for a cantilever supporting a lumped mass.

002x002.eps

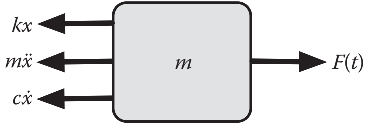

Figure 2.3 Dynamic equilibrium using d'Alembert's principle.

002x003.eps

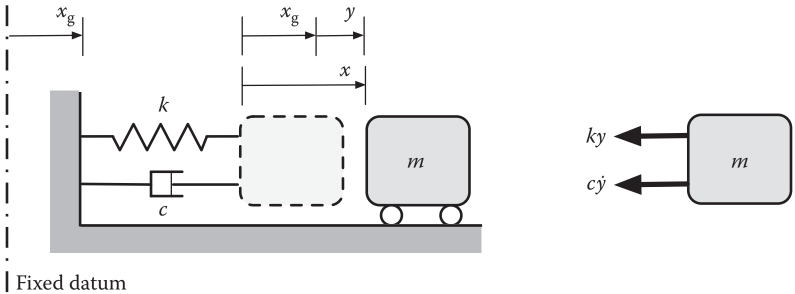

Figure 2.4 Damped SDOF system subjected to a base motion.

002x004.eps

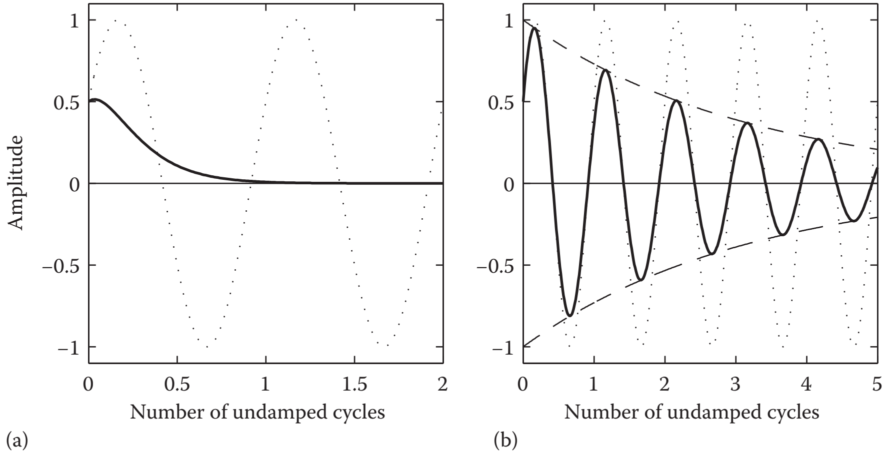

Figure 2.5 Damped free vibrations: (a) critically damped, (b) with 5% critical damping. Both cases have the same initial displacement and velocity. The undamped response is shown dashed.

002x005.eps

Courtesy of CRC Press/Taylor & Francis Group

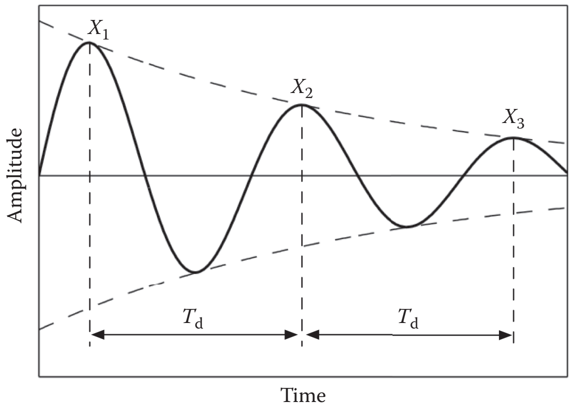

Figure 2.6 Viscously damped free vibrations giving a constant amplitude ratio between successive peaks.

002x006.eps

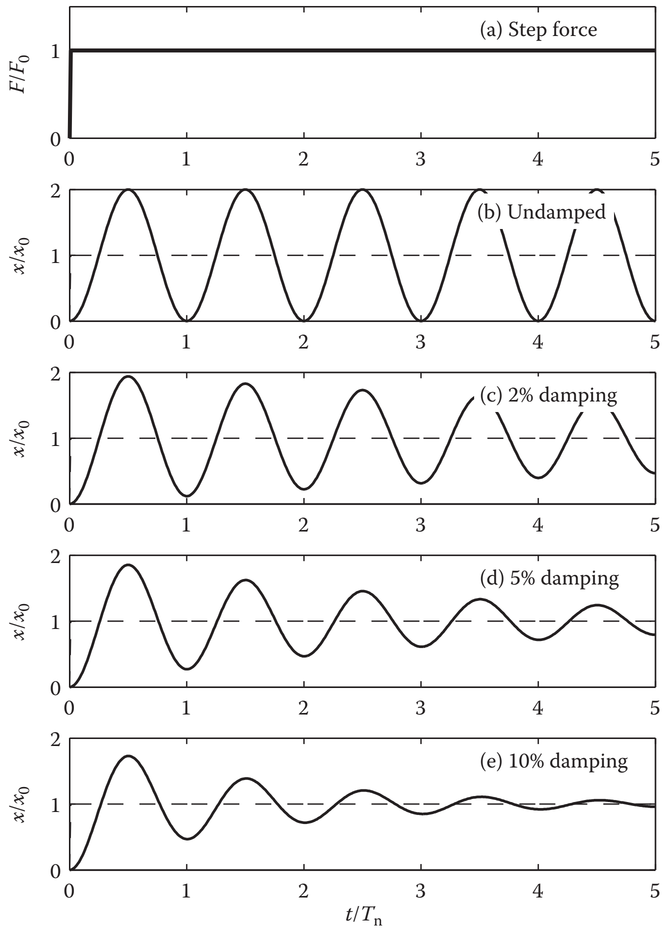

Figure 2.7 Vibration of an SDOF system in response to a step load, for various levels of damping (static response x_0 shown dashed).

002x007.eps

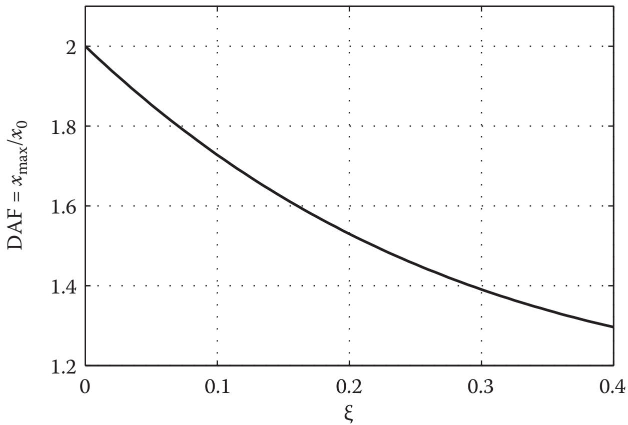

Figure 2.8 Dynamic amplification factor for an SDOF system responding to a step load, as a function of the damping ratio.

002x008.eps

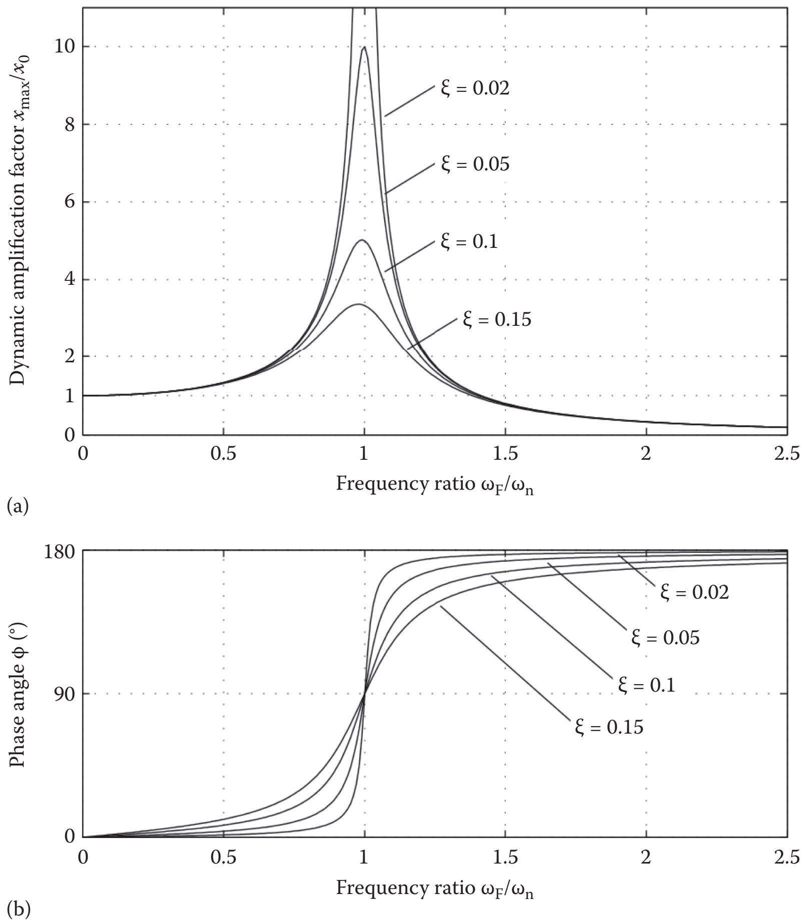

Figure 2.9 (a) Dynamic amplification factor and (b) phase angle for steady state response of an SDOF system to a harmonic force, as a function of the frequency ratio.

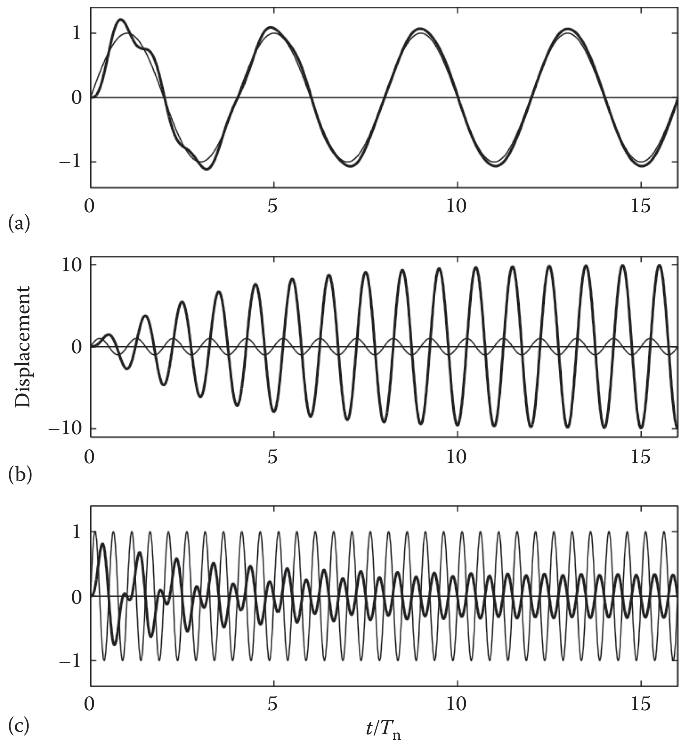

Figure 2.10 Time histories of displacement response of a 5% damped SDOF system to a unit-amplitude harmonic load. The frequency ratio is (a) 0.25 – quasi-static loading, (b) 1.0 – resonance, and (c) 2.0 – fast loading. The thin line is the static displacement (F/k) and the heavy line the dynamic response.

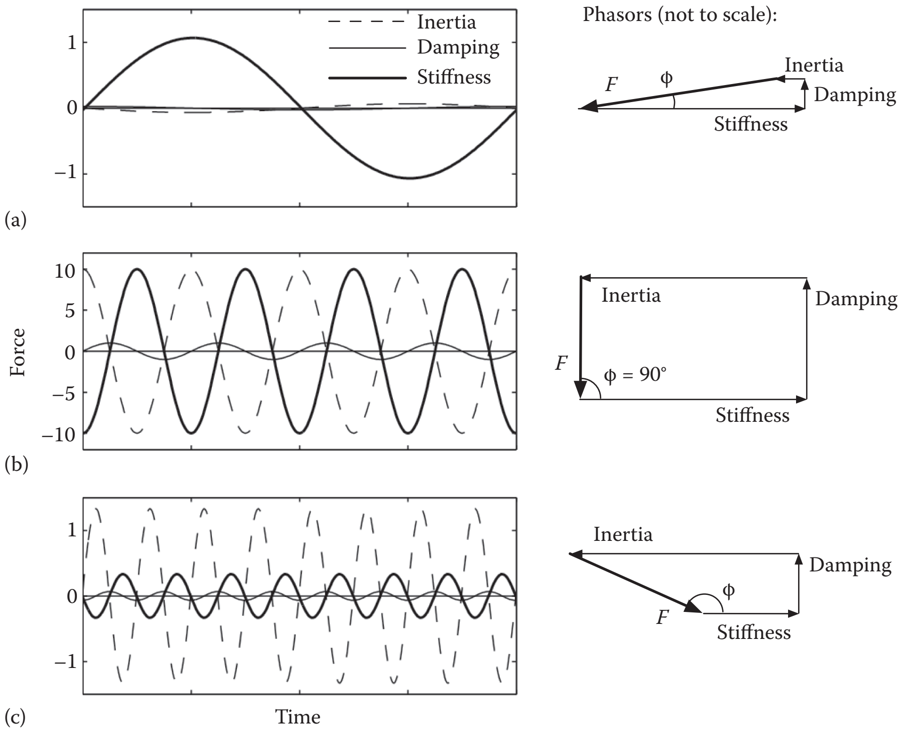

Figure 2.11 Time histories and phasor representation (not to scale) of inertia, damping and stiffness force components for a 5% damped SDOF system subjected to a unit-amplitude harmonic load, with frequency ratio (a) 0.25, (b) 1.0, (c) 2.0.

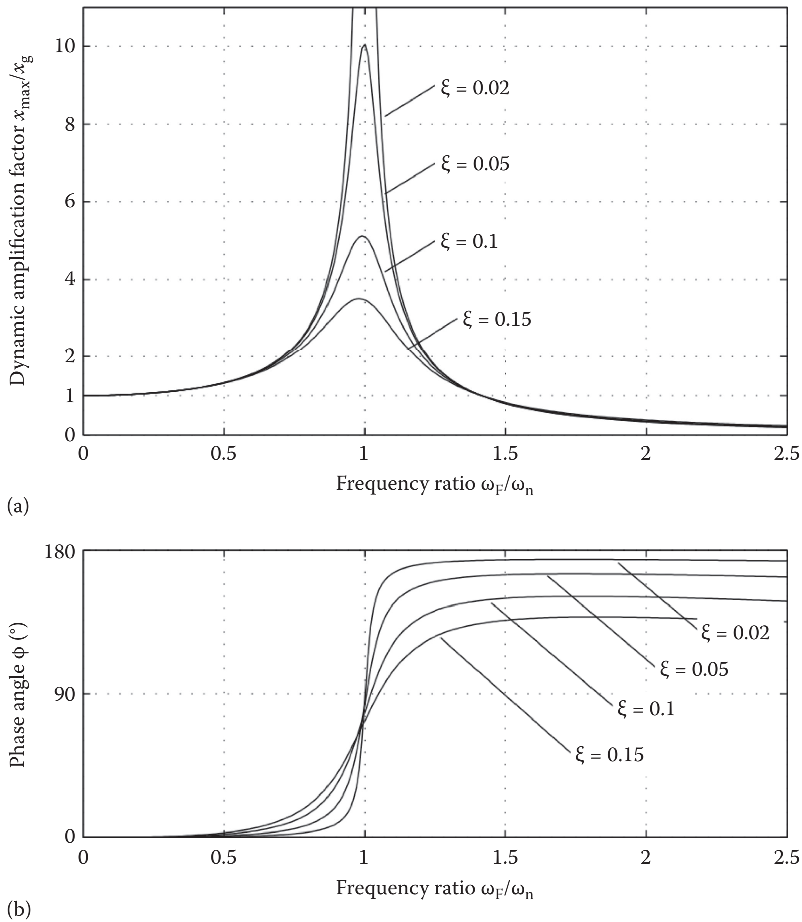

Figure 2.12 (a) Dynamic amplification factor and (b) phase angle for steady state response of an SDOF system to a harmonic base motion, as a function of the frequency ratio.

002x012.eps

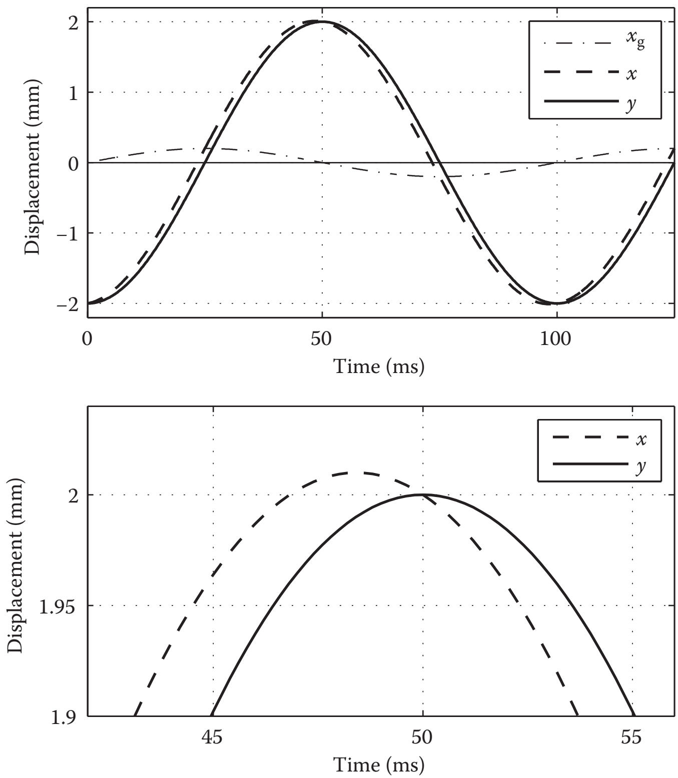

Figure 2.13 A typical part of the absolute (x) and relative (y) steady state displacements of an SDOF structure in response to a harmonic base motion x_g. The lower plot is a zoom of the peak, to show more clearly the small amplitude and phase differences between x and y.

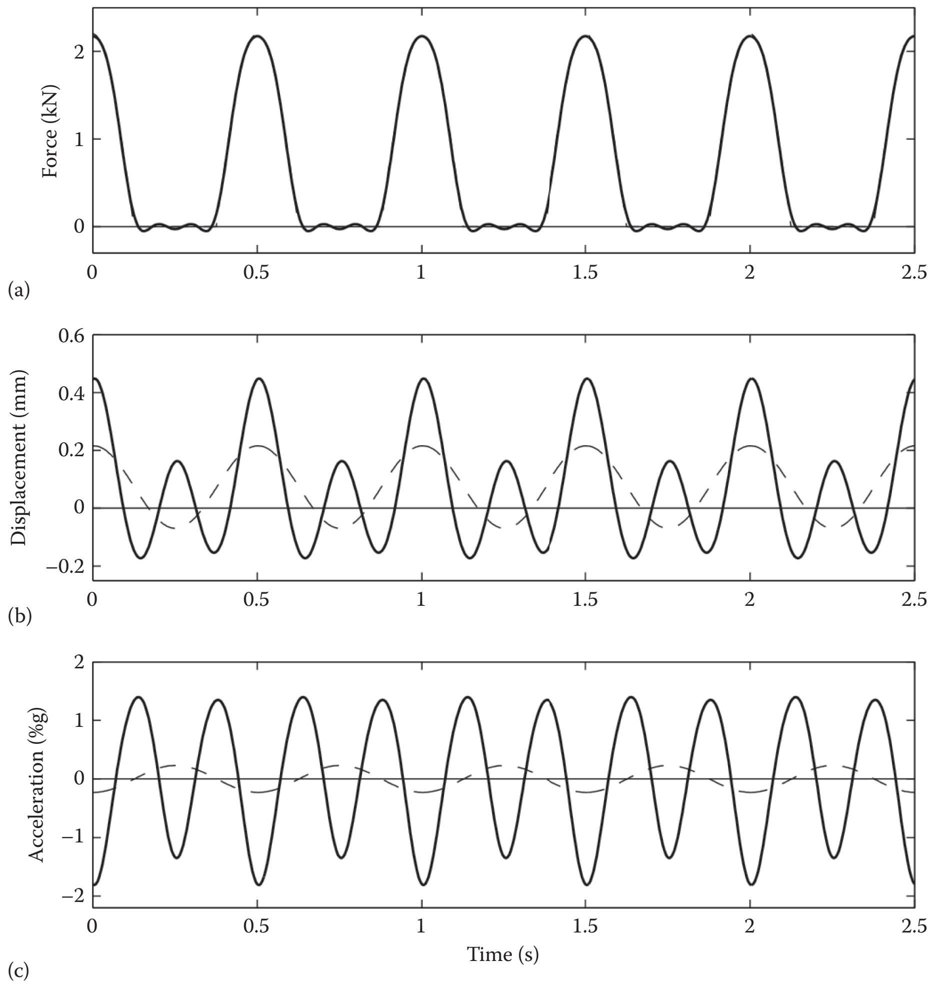

Figure 2.14 Effect of jumping on a floor: (a) idealised jumping force time history and its approximation by Fourier series terms up to the fourth harmonic, (b) resulting floor displacement, (c) floor acceleration. In (b) and (c), the solid line is calculated using terms up to the fourth harmonic, the dashed line using the first harmonic only.

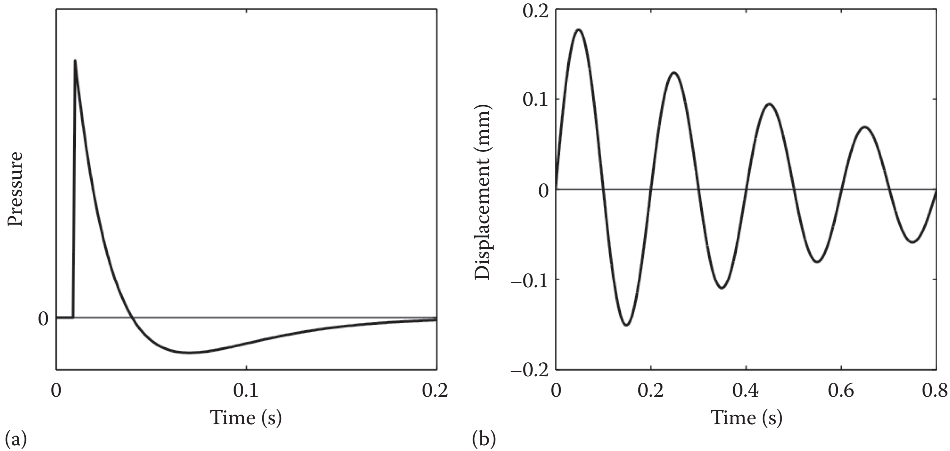

Figure 2.15 Response of an SDOF structure to a blast wave: (a) typical blast pressure time history (idealised as an instantaneous impulse in this analysis), (b) displacement response.

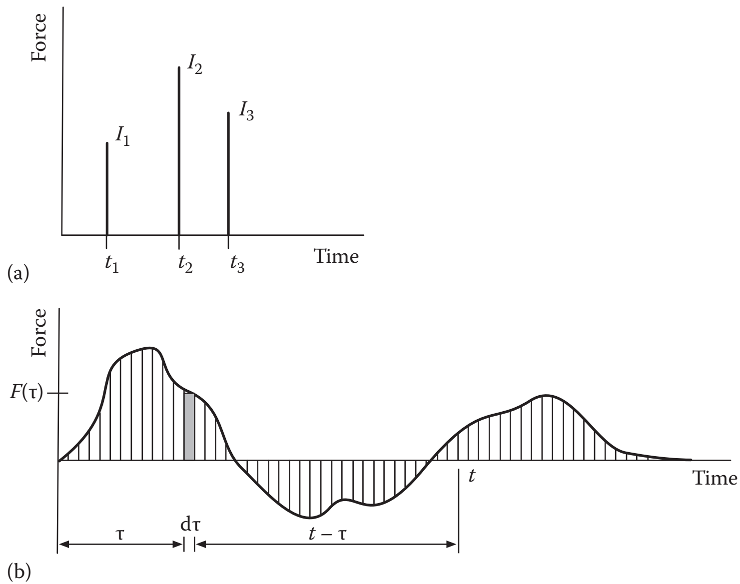

Figure 2.16 Treating irregular loads as sums of impulses: (a) three short pulses, (b) discretisation of a continuous load, leading to Duhamel's integral.

002x016.eps

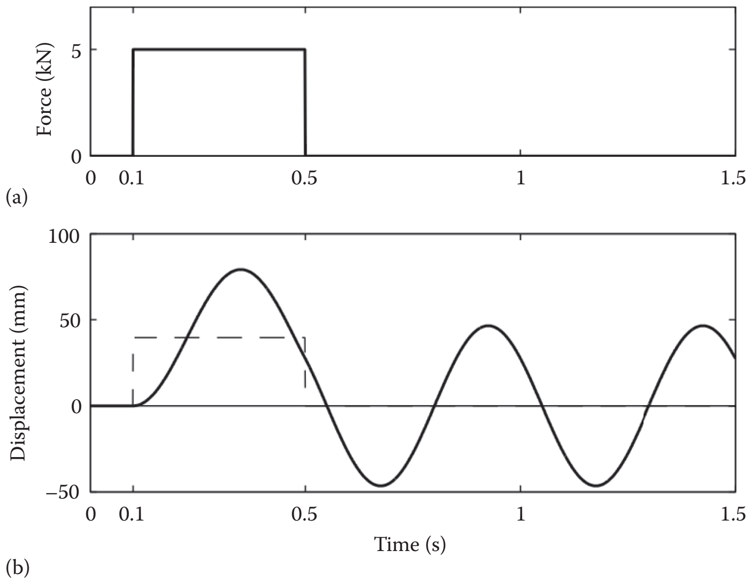

Figure 2.17 (a) Short-duration step load and (b) displacement response of undamped SDOF system as calculated by Duhamel's integral (static response shown dashed).

002x017.eps

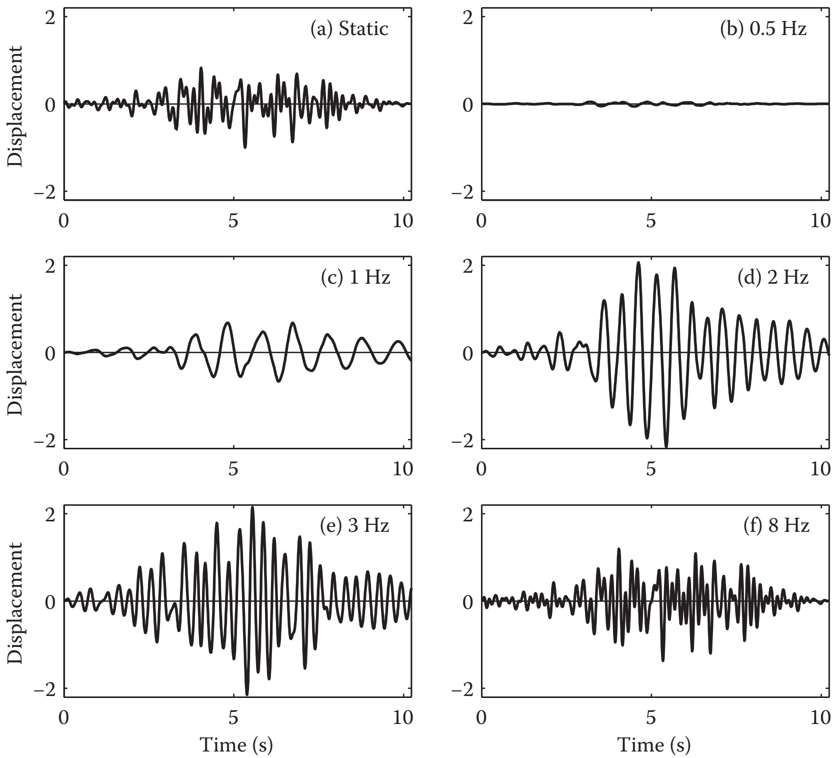

Figure 2.18 Time history responses of 5% damped SDOF systems computed by Duhamel's integral. The input force has frequency components evenly distributed in the range 1–6 Hz. (a) shows the static displacement F/k, while (b)–(f) show responses of oscillators with different frequencies. The displacement axes are normalised to give a peak static displacement of 1.

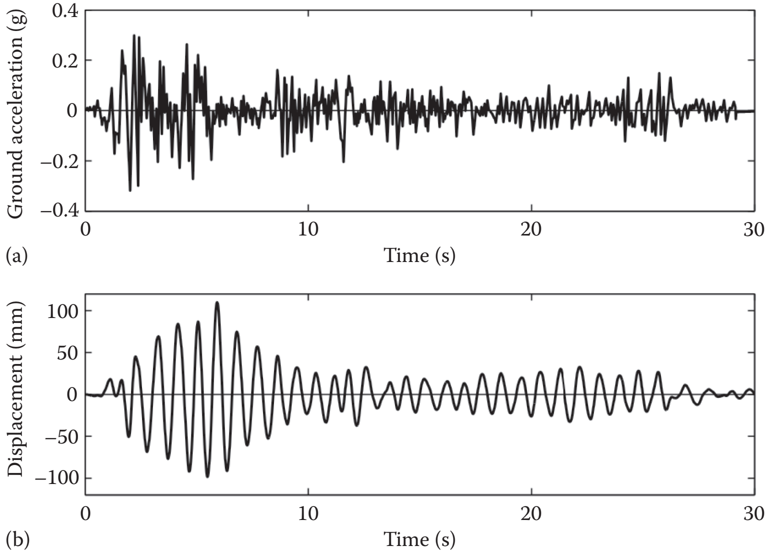

Figure 2.19 Response of a 5% damped SDOF system to the 1940 El Centro earthquake: (a) ground acceleration (g), (b) displacements (mm) computed by Duhamel's integral.

002x019.eps

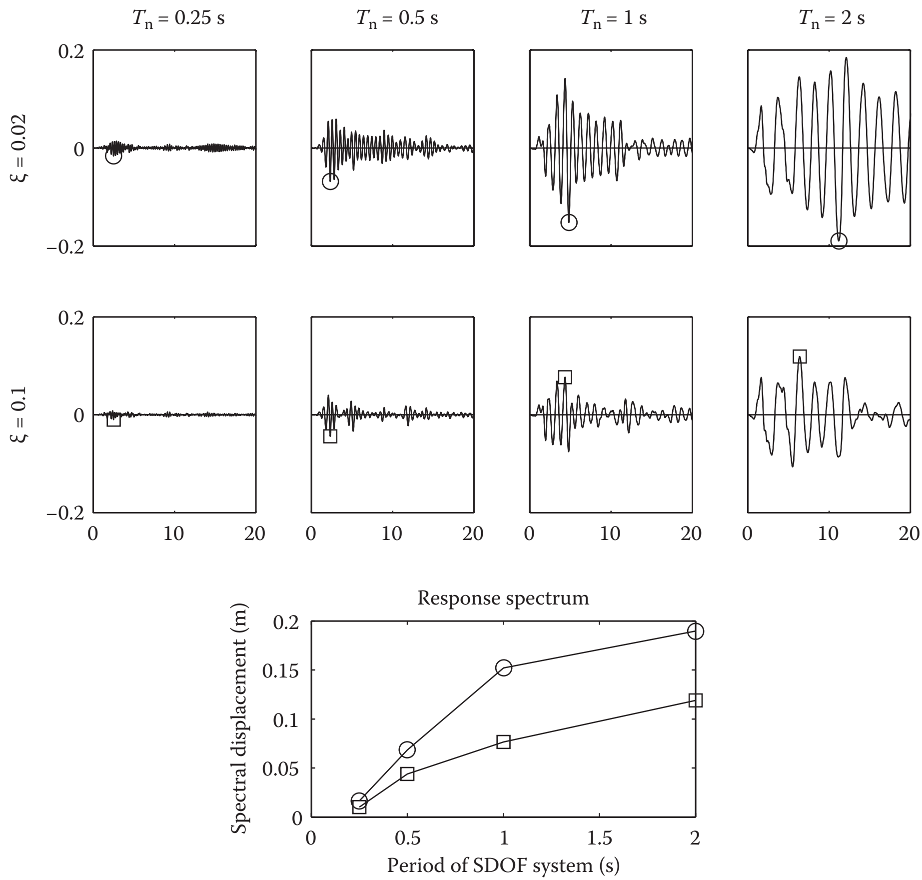

Figure 2.20 Construction of a response spectrum for the El Centro earthquake: the upper graphs plot displacement (m) versus time (s) for SDOF systems having four different natural periods and two damping ratios. The peak absolute values are then plotted against the natural period to form the spectrum in the bottom graph.

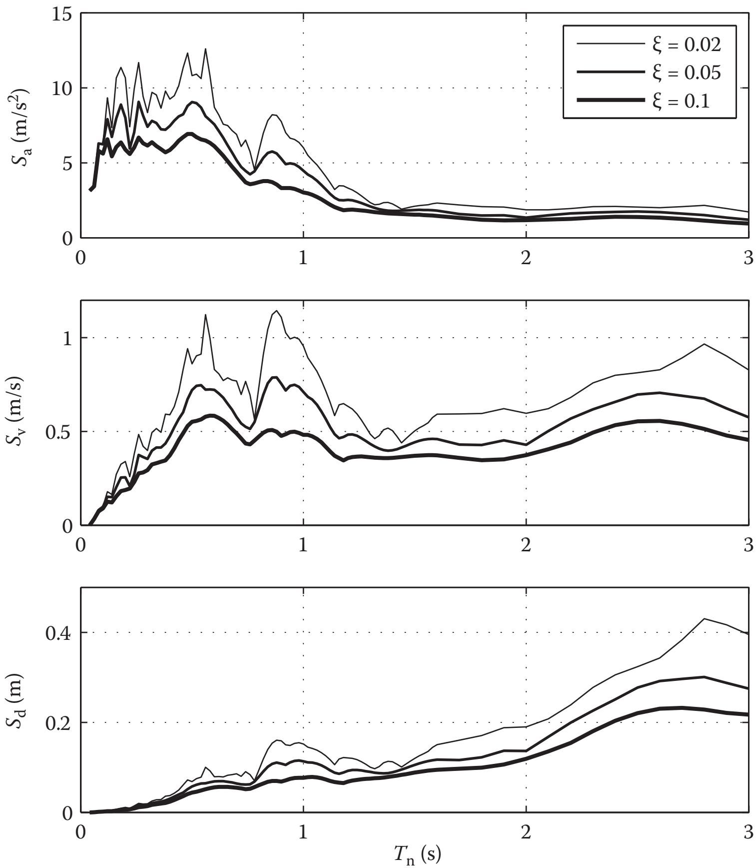

Figure 2.21 Acceleration, velocity and displacement response spectra for the El Centro earthquake at three damping levels.

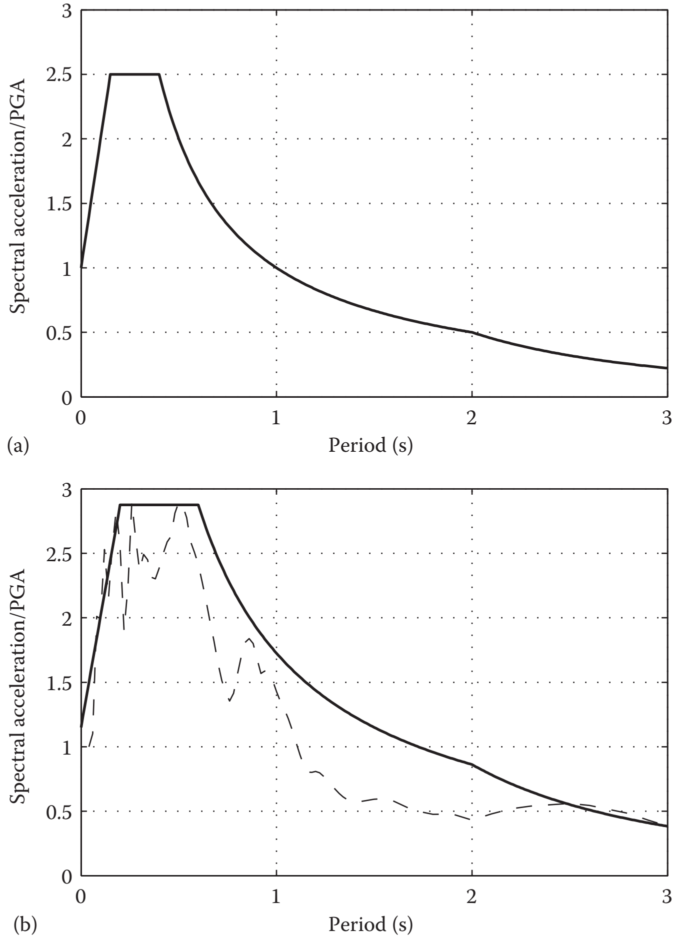

Figure 2.22 Examples of Eurocode 8 Type I acceleration response spectra for 5% damped structures. (a) Structures on ground type A – rock, (b) structures on ground type C – stiff soil, also showing 5% damped El Centro spectrum for comparison.

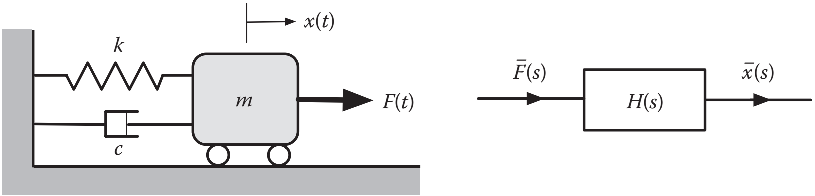

Figure 2.23 An SDOF system and the block diagram representation of its transfer function.

002x023.eps

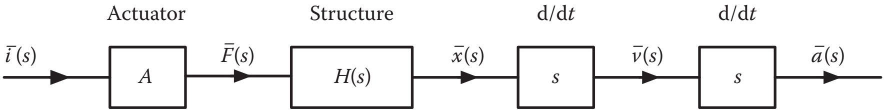

Figure 2.24 Block diagram representation of an SDOF structure loaded by an actuator.

002x024.eps

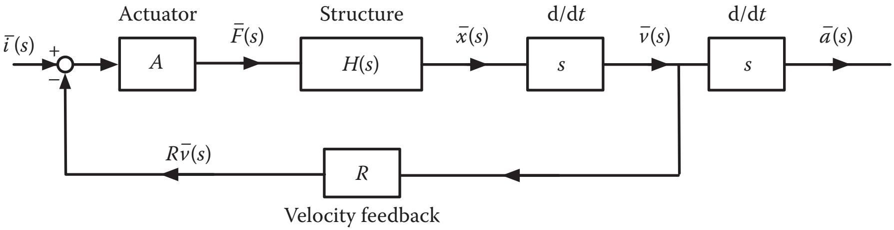

Figure 2.25 Modifying a block diagram by a velocity feedback loop.

002x025.eps

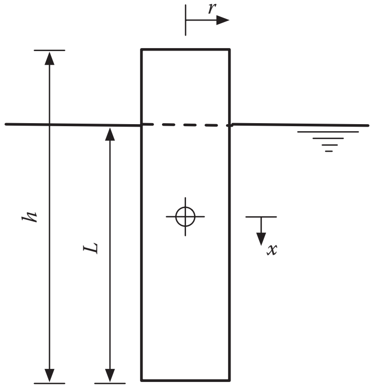

Figure P2.2

PRB002x002.eps

Courtesy of CRC Press/Taylor & Francis Group

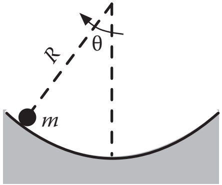

Figure P2.3

PRB002x003.eps

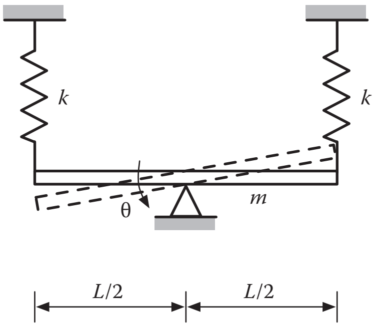

Figure P2.4

PRB002x004.eps

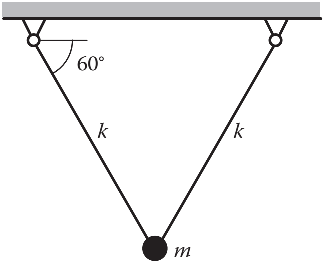

Figure P2.5

PRB002x005.eps

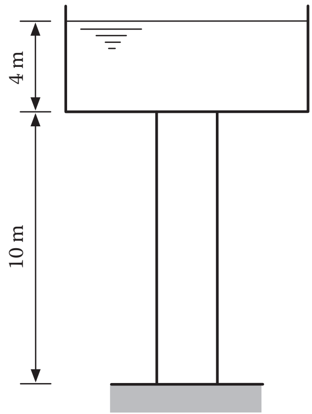

Figure P2.11

PRB002x011.eps